DISPERSION CHARACTERISTICS OF FIBER-REINFORCED PRESTRETCHED MATERIALS: A SAFE APPROACH

ASESH KUMAR PATRA*, ROHAN S. SAPRU AND M. M. JOGLEKAR

Department of Mechanical and Industrial Engineering,
Indian Institute of Technology Roorkee 247667, India
akumarpatra@me.iitr.ac.in

Keywords: Smart materials, Hyperelasticity, Wave propagation, Numerical framework, Strain stiffening effect, Anisotropy

Abstract. The expanding realm of compliant and flexible soft solids is marked by notable advantages, offering secure interactions with humans and delicate objects. This study employs advanced numerical methodologies to meticulously investigate the propagation of elastic plate waves within a fiber-reinforced prestretched compressible material, characterized by the Gent hyperelasticity model. The formulation encompasses the elastic tensor and underlying wave equations in Lagrangian space, integrating the theory of nonlinear elasticity with linearized incremental equations. To compute the dispersion characteristics of two fundamental guided wave modes, an extension of the Semi-Analytical Finite Element (SAFE) method is introduced. Subsequently, the investigation delves into the intricate effects of applied prestretch, reinforced fiber orientation, and material parameters on the dispersion characteristics of fundamental Lamb modes. A limiting case of the neo-Hookean material model is scrutinized to elucidate implicit dependencies, with a specific emphasis on the strain-stiffening effect captured through the Gent material model. The study's findings unveil that the manipulation of material anisotropy and fiber direction provides precise control over anti-symmetric and symmetric modes. The comprehensive exploration and insights presented in this study significantly contribute to the understanding and control of wave propagation in hyperelastic materials, particularly those exhibiting Gent- type behavior.

1 INTRODUCTION

Recently, there has been growing interest in studying wave propagation through nonlinear hyperelastic materials. Hyperelastic materials are a class of nonlinear elastic materials that can undergo large reversible deformations with little change in applied stress. Examples of hyperelastic materials include rubbers, elastomers, soft polymers, and biological tissues[1, 2]. Guided ultrasonic waves such as Lamb modes offer a powerful tool for non-destructively probing the structural health of plate and shell type structures [3]. But the propagation of such waves in deformed transversely isotropic hyperelastic media remains relatively unexplored, restricting defect detection and health monitoring applications. The development of a robust analytical framework can pave the way for novel non-destructive analysis in diverse areas ranging from flexible structural components to biological tissues.

   Most existing literature has utilized analytical approaches to study guided wave behaviour in finitely stretched materials, primarily on linearly elastic materials, providing limited physical insights. Study of small amplitude Rayleigh waves through isotropic, elastic material can be traced back to the articles [4, 5] in which the theory of superposition of infinitesimal deformations on finite deformations was applied to a semi-infinite body with an initial homogeneous deformation. Development of finite deformation theory [6] helped in incorporating effects of non-linear elasticity in such studies. [7] showed that shear waves can be used to measure the third and fourth order elastic constants of incompressible soft solid through their coupling with pre-deformation. In the same article, it is shown

that wave propagation through pre-stretched non linearly elastic plates can be approached in two methods. The first method is the theory of exact non-linearity which is applied for finite deformations to study elastic wave propagation through highly deformable elastomers and soft solids like human tissues which is explained in [8] where incremental small, time dependant displacements are superimposed on the finite deformation of a incompressible, isotropic elastic material. Frequencies of the different symmetric and anti-symmetric modes of wave in terms of underlying deformation and stress were found and frequencies of the different symmetric and anti-symmetric modes of wave in terms of underlying deformation and stress were found. The strain energy functions were written in terms of first three invariants of Cauchy-Green strain tensor. The dispersion effects of small amplitude waves propagating along non-principal direction in a compressible pre-stressed elastic plate was studied in [9, 10]. The second approach is the theory of weakly non-linear elasticity is usually used in the study of small but not infinitesimal deformations. In this approach, the strain energy density function is represented in terms of Green-Lagrange strain tensor. The equations of acoustoelasticity for shear waves propagating through orthotropic elastic materials with pre-stress are derived in [11].

Acoustoelasticity of Lamb waves propagating through bi-axially stressed isotropic material was studied in [12] using the technique of superposition of partial bulk waves (SPBW) which is a matrix based approach in order to solve the non-linear algebraic for the dispersion plots which was found to change anisotropically for most stresses, modes and frequencies although there are some frequency-mode combinations dispersion is isotropic in nature. SPBW methods rely on complex bidirectional root-searching algorithms to handle solutions with complex wave numbers, such as damped waveguides. However, as shown in [13], these algorithms can sometimes miss certain solutions entirely. This possibility of overlooked solutions is a significant downside to using the SPBW approach for problems involving damping. The Semi-Analytical Finite Element (SAFE) method has emerged as a useful alternative to the SPBW technique, as it overcomes limitations of SPBW approach. Rather than using a complex root-searching process like in SPBW, SAFE solves eigenvalue problems in a stable way to produce dispersion characteristics. In terms of implementation, SAFE uses a finite element discretization of the waveguide cross-section and presumes the solution varies harmonically in both time and the direction of propagation. This lowers the dimensionality of the problem, cutting down computational costs [3, 21, 22]. SAFE is used in [14, 15] to model the dispersion characteristics of guided waves propagating through materials of arbitrary cross-sections which are subjected to axial loads while viscoelastic effects were added in [3] for linearly elastic material. Dispersion curves of Lamb waves for a weakly non-linear plate is discussed in [16] where the results were validated by using the analytical method of SPBW. Similar study has been performed by [17] where isotropic Gent model was taken as the specimen. Different types of strain energy functions for anisotropic Gent model have been discussed in [18, 23, 24]. However, analyzing wave dispersion in such materials under finite deformation poses theoretical and computational challenges. This paper aims to develop a numerical framework for characterizing guided Lamb waves traveling through a pre-stretched transversely isotropic hyperelastic plate based on SAFE approach.

This paper is structured as follows: Section 2 explains the formulations involved in the problem which is divided into sub-sections: Section 2.1 starts with brief discussion on theory of non-linear elasticity of pre-stretched transversely isotropic hyperelastic plates and later presents the derivation of elastic moduli for the model. In Section 2.2, SAFE formulations are presented for the model which helps in the calculation of the phase velocity of different modes of the Lamb waves propagating through the plate. Section 3 presents the effects of varying pre-stretches and other material parameters on the dispersion behaviour of the model. Finally, conclusions and future prospects are provided in Section 4.

2   FORMULATIONS OF THE PROBLEM

For simplicity, the formulation is split into two parts: first, the equations for the elastic moduli are

developed for transversely isotropic hyperelastic materials with one family of fibers. Second, the semi-analytical finite element method is presented to solve the wave propagation problem using the elastic moduli.

2.1 Derivation of elastic moduli

For the purpose of studying elastic materials exhibiting non-linear mechanical properties, we define a strain energy function (W) to represent in terms of energy its mechanical behaviour. A material is called elastic when W exists such that the stress can be obtained by differentiating W with respect to the strain. Such relations between strain and stress are called constitutive relations which describe the macroscopic behaviour of a material.

For isotropic materials, the stress-strain relation has to be independent of the co-ordinate system used since the material has same properties in all directions. Hence, the strain energy function is defined using invariants of strain or that of deformation tensor. If undeformed state is used as frame of reference, the three invariants of right Cauchy-Green deformation tensor $\mathbf{C}$ are given as

$$I_1 = \text{tr}\,(\mathbf{C}) = \lambda_1^2 + \lambda_2^2 + \lambda_3^2 \tag{1}$$

$$I_2 = \frac{1}{2}[(\text{tr}\,\mathbf{C})^2 - \text{tr}\,(\mathbf{C}^2)] = \lambda_1^2\lambda_2^2 + \lambda_2^2\lambda_3^2 + \lambda_3^2\lambda_1^2 \tag{2}$$

$$I_3 = \det\,\mathbf{C} = \lambda_1^2\lambda_2^2\lambda_3^2 \tag{3}$$

where λ_1^2, λ_2^2, λ_3^2 are the eigenvalues of $\mathbf{C}$. From polar decomposition, it can be shown that the λ_1, λ_2, and λ_3 are eigenvalues of left stretch tensor $\mathbf{U}$, also known as principal stretches.

Let us consider a deformable, compressible transversely isotropic hyperelastic body. The body is considered to be transversely isotropic because of the presence of one family of unidirectional fibers in an isotropic matrix. Let us assume that the body is described by the region π_0 in the undeformed state which is also taken as the reference state while it is described by the region π_r in the deformed state which is also the current state of the body. The two states are defined using the coordinate systems ξ and x respectively.

The body is considered to be a hyperelastic plate with dimensions L, B and H in the reference coordinate system (ξ_1, ξ_2, ξ_3) as shown in Figure 1. Assume that due to an external uniaxial load in the ξ_1 direction, the body has undergone a finite deformation whose current dimension are now $\lambda_1 L$, $\lambda_2 B$ and $\lambda_3 H$ in the current coordinate system (x_1, x_2, x_3). λ_1, λ_2 and λ_3 are the principal pre-stretches in the reference coordinate system. Both the coordinate axes coincide with each other and are attached to mid-plane of the plate.

Using the Lagrangian motion description, current spatial coordinates can be written in terms of the reference spatial coordinates as:

$$x_1 = \lambda_1\xi_1, x_2 = \lambda_2\xi_2, x_3 = \lambda_3\xi_3 \tag{4}$$

Second order tensor deformation gradient is defined in Einstein notation as:

$$F_{\alpha j} = \frac{\partial x_\alpha}{\partial \xi_j} \tag{5}$$

where $\alpha, j = 1, 2, 3$. In this study, we take lowercase English alphabets to represent directions in the

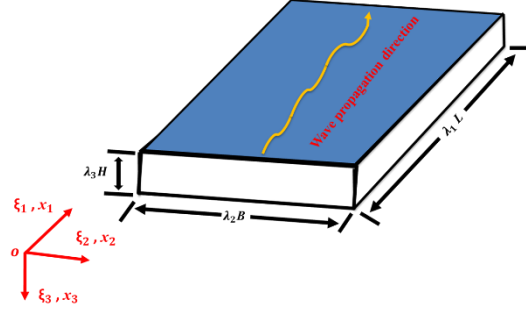reference state while the current state is represented by Greek alphabets.

Figure 1: Schematic of the plate in the deformed state.

Using (2) we can write the deformation gradient for our problem as,

$$F_{\alpha q} = \begin{bmatrix} \lambda_1 & 0 & 0 \\ 0 & \lambda_2 & 0 \\ 0 & 0 & \lambda_3 \end{bmatrix} \tag{6}$$

The right Cauchy-Green deformation tensor and Green strain tensor is defined by equations 7 and 8 respectively.

$$C_{ij} = F_{\gamma i} F_{\gamma j} \tag{7}$$

$$E_{ij} = \frac{1}{2} (C_{ij} - \delta_{ij}) \tag{8}$$

where δ_{ij} is Kronecker delta.

The strain energy density function (W) for compressible transversely isotropic Gent model applied in this problem is:

$$W = \frac{-\mu j_m}{2} \ln \left(1 - \frac{I_1 - 3}{j_m} \right) - \mu \ln J + \left(\frac{\lambda_m}{2} - \frac{\mu}{j_m} \right) (J - 1)^2 + \frac{\mu}{2} \xi (I_4 - 1)^2 \tag{9}$$

where μ is infinitesimal initial shear modulus, j_m is a dimensionless parameter called Gent constant which is a measure of the strain stiffening effect in the model, J is termed as Jacobian which represents ratio of current volume to initial (or reference) volume, ξ is the degree of anisotropy and I_4 is the additional anisotropic invariant defined as $I_4^{(\alpha)} = \boldsymbol{a}_0^{(\alpha)} \cdot \mathbf{C} \cdot \boldsymbol{a}_0^{(\alpha)}$;

α = 1,2…. N, N is the total family of fibers present. $\boldsymbol{a}_0^{(\alpha)}$ is the unit vector representing the orientation of fibers with respect to the x_1 direction as shown in Figure 2.[18]
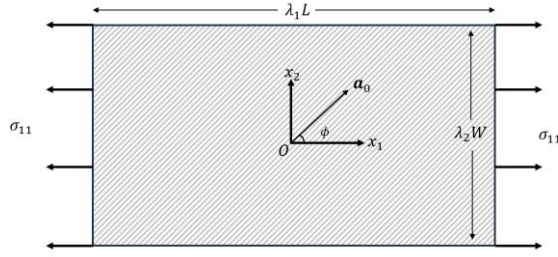
Figure 2: Schematic of a deformed, anisotropic, hyperelastic membrane

Different stresses induced at a point inside a body undergoing finite deformation is given by,
First Piola–Kirchhoff Stress

$$P_{\alpha j} = \frac{\partial W}{\partial F_{\alpha j}} \tag{10}$$

Second Piola-Kirchhoff Stress

$$S_{ij} = 2\frac{\partial \psi}{\partial C_{ij}} \tag{11}$$

Cauchy Stress

$$\sigma_{\alpha \beta} = J^{-1}F_{\alpha l}S_{lk}F_{\beta k} = J^{-1}P_{\alpha k}F_{\beta k} \tag{12}$$

First and second Piola-Kirchhoff stresses are calculated based on area of cross-section in reference coordinate system while Cauchy stress is defined w.r.t area in the current coordinate system.

By substituting the (9) in equation (12), the components of the Cauchy stress can be formulated as:

$$\sigma_{11} = \frac{\lambda_1}{\lambda_2 \lambda_3}\left[\frac{\mu j_m}{j_m - \lambda_1^2 - \lambda_2^2 + \lambda_3^2 + 3}\right] + 2\left(\frac{\lambda_m}{2} - \frac{\mu}{j_m}\right)(\lambda_1 \lambda_2 \lambda_3 - 1) - \frac{\mu}{\lambda_1 \lambda_2 \lambda_3} \tag{13}$$
$$+ 2\mu\xi \cos^2(\phi)\,(\lambda_1^2 \cos^2(\phi) + \lambda_2^2 \sin^2(\phi) - 1)$$

$$\sigma_{22} = \frac{1}{\lambda_1}\left[\frac{\mu j_m}{j_m - \lambda_1^2 - \lambda_2^2 + \lambda_3^2 + 3}\right] + 2\left(\frac{\lambda_m}{2} - \frac{\mu}{j_m}\right)(\lambda_1 \lambda_2 \lambda_3 - 1) - \frac{\mu}{\lambda_1 \lambda_2 \lambda_3} \tag{14}$$
$$+ 2\mu\xi \sin^2(\phi)(\lambda_1^2 \cos^2(\phi) + \lambda_2^2 \sin^2(\phi) - 1)$$

$$\sigma_{33} = \frac{1}{\lambda_1}\left[\frac{\mu j_m}{j_m - \lambda_1^2 - \lambda_2^2 + \lambda_3^2 + 3}\right] + 2\left(\frac{\lambda_m}{2} - \frac{\mu}{j_m}\right)(\lambda_1 \lambda_2 \lambda_3 - 1) - \frac{\mu}{\lambda_1 \lambda_2 \lambda_3} \tag{15}$$

$$\sigma_{12} = \sigma_{21} = \frac{2\mu\xi\cos(\phi)\sin(\phi)(\lambda_1^2\cos^2(\phi) + \lambda_2^2\sin^2(\phi) - 1)}{\lambda_3}F_{\beta k} \tag{16}$$

For a known value of λ_1 i.e., the pre-stretch in the direction of uniaxial load, using (13) – (16), we can calculate the pre-stretches in the other two directions, due to Poisson's effect, λ_2, λ_3 as well as the tensile stress and shear stress induced in the body due to the load.

Using the Lagrangian form of incremental governing equation explained in [19],

$$\text{Div } \dot{P} = \rho° v, tt \tag{17}$$

where $\dot{P}$ is the nominal stress and v is the incremental displacement. $\rho°$ is the density of the material in the reference coordinate system.

The incremental nominal stress is related to the elastic modulus of the body in the Lagrangian space as:

$$\dot{P}_{\alpha j} = B_{\alpha j \gamma l} v_{\gamma, l}, \tag{18}$$

where $B_{\alpha j \gamma l}$ represents the elastic moduli of the body and is given by,

$$B_{\alpha j \gamma l} = 4 F_{\alpha i} F_{\gamma k} \frac{\partial^2 W}{\partial C_{ij} \partial C_{kl}} + S_{jl} \delta_{\alpha \gamma} \tag{19}$$

where,

$$\frac{\partial^2 W}{\partial C_{ij} \partial C_{kl}} = \frac{1}{4} \left[\frac{2 \mu j_m}{(j_m - I_1 + 3)^2} \delta_{ij} \delta_{kl} - \left(2 \left(\frac{\lambda_m}{2} - \frac{\mu}{j_m} \right) * (J^2 - J) - \mu \right) \left(C_{ik}^{-1} C_{jl}^{-1} + C_{il}^{-1} C_{jk}^{-1} \right) + 2J(J - 1) \left(\frac{\lambda_m}{2} - \frac{\mu}{j_m} \right) C_{ij}^{-1} C_{kl}^{-1} + 4 \mu \xi a_i a_j a_k a_l \right]$$

$$S_{jl} = 2 \frac{\partial W}{\partial C_{jl}} = \frac{\mu j_m}{(j_m - I_1 + 3)} \delta_{jl} + \left(2 \left(\frac{\lambda_m}{2} - \frac{\mu}{j_m} \right) (J^2 - J) - \mu \right) C_{jl}^{-1} + 2 \mu \xi (I_4 - 1) a_j a_l$$

$$\vec{a} = \{\cos \phi \quad \sin \phi \quad 0\}^T$$

Substituting (18) in (19), we get,

$$B_{\alpha j \gamma l} \frac{\partial^2 v_\gamma}{\partial \xi_j \partial \xi_l} = \rho° \frac{\partial^2 v_\alpha}{\partial t^2} \tag{20}$$

2.2 Semi analytical finite element method formulation

The elastic moduli from Section 2.1 are used in semi analytical finite element method to get the dispersion plots of small amplitude guided plate waves propagating through the pre-stretched anisotropic hyperelastic plate. It is also assumed that the Lamb wave is propagating in the direction ξ_1 and that the attenuation to the wave is negligible.

To solve the incremental governing equation (20), we have to also consider the boundary conditions. i.e., the traction at the upper ($\xi_3 = -H/2$) and lower ($\xi_3 = H/2$) surfaces of the hyperelastic plate are taken to be zero in both reference and current coordinate system which can be written in the Lagrangian form as:

$$t_\alpha = \dot{P}_{\alpha j} n_j = 0 \tag{21}$$

The weak form of the governing equation is given by,

$$\int_{\pi_o} \delta v_\alpha B_{\alpha j \gamma l} v_{\gamma, lj} dV = \int_{\pi_o} \delta v_\alpha \rho° v_{\alpha, tt} dV \tag{22}$$

where δv_α is the virtual displacement. Applying integration by parts at LHS of (22) and expanding we get,

$$\int_{\pi_o} \delta v_{\alpha,j} B_{\alpha j\gamma l} v_{\gamma,l} dV + \int_{\pi_o} \delta v_\alpha \rho^o v_{\alpha,tt} dV = \int_{\Gamma_o} \delta v_\alpha t_\alpha dS \tag{23}$$

Γ_o is the surface boundary of the domain π_o. RHS of the equation (23) will be zero because of the absence of traction at the top and bottom surface. In SAFE framework, the component of displacement in the direction of wave propagation will be substituted by the value obtained from analytical method which is a harmonic exponential function in this case and components along the cross section perpendicular to wave propagation will be approximated by finite element methods. The waves propagating through the body are plane waves with wave number k and frequency ω and is independent of the displacement in the direction of ξ_2 axis. Hence, the problem is simplified to a 1D system with thickness of the plate as the domain which is discretized by three node 1D elements. The resulting displacement vector becomes:

$$v = \{v_1(\xi_1,\xi_3)\ v_2(\xi_1,\xi_3)\ v_3(\xi_1,\xi_3)\}^T \tag{24}$$

$$\frac{\partial v}{\partial \xi} = \left\{ \frac{\partial v_1}{\partial \xi_1} \frac{\partial v_2}{\partial \xi_2} \frac{\partial v_3}{\partial \xi_3} \frac{\partial v_1}{\partial \xi_2} \frac{\partial v_1}{\partial \xi_3} \frac{\partial v_2}{\partial \xi_1} \frac{\partial v_2}{\partial \xi_3} \frac{\partial v_3}{\partial \xi_1} \frac{\partial v_3}{\partial \xi_2} \right\}^T \tag{25}$$

$$= \left\{ L_1 \frac{\partial}{\partial \xi_1} + L_3 \frac{\partial}{\partial \xi_3} \right\}^T v$$

where $\quad L_1 = \begin{bmatrix} 1 & 0 & 0 \\ 0 & 0 & 0 \\ 0 & 0 & 0 \\ 0 & 0 & 0 \\ 0 & 0 & 0 \\ 0 & 1 & 0 \\ 0 & 0 & 0 \\ 0 & 0 & 1 \\ 0 & 0 & 0 \end{bmatrix}$ and $L_3 = \begin{bmatrix} 0 & 0 & 0 \\ 0 & 0 & 0 \\ 0 & 0 & 1 \\ 0 & 0 & 0 \\ 1 & 0 & 0 \\ 0 & 0 & 0 \\ 0 & 1 & 0 \\ 0 & 0 & 0 \\ 0 & 0 & 0 \end{bmatrix}$.

The displacement can be expressed as:

$$v = N v^e e^{i(k\xi_1 - \omega t)} \tag{26}$$

$$v^e = (v_{11}^e \quad v_{22}^e \quad v_{33}^e \quad v_{12}^e \quad v_{13}^e \quad v_{21}^e \quad v_{23}^e \quad v_{31}^e \quad v_{32}^e)^T \tag{27}$$

$$\int_{\pi_o} \delta v_{\alpha,j} B_{\alpha j\gamma l} v_{\gamma,l} dV + \int_{\pi_o} \delta v_\alpha \rho^o v_{\alpha,tt} dV = \int_{\Gamma_o} \delta v_\alpha t_\alpha dS \tag{28}$$

where v_{ij}^e is the nodal displacement of the ith node along the direction of axis j in the reference state. N is the shape function matrix with N$_1$, N$_2$ and N$_3$ being the corresponding shape functions of three nodes in the element.

From (26),

$$\frac{\partial v}{\partial \xi} = [A_1 + ikA_2]v^e e^{i(k\xi_1 - \omega t)} \tag{29}$$

where $A_1 = L_3 \frac{\partial N}{\partial \xi_3}$ and $A_2 = L_1 N$.

The above expressions can be substituted in the weak form which will give,

$$\int_{\pi_o} \delta v^{eT}[A_1^T - ikA_2^T][B][A_1 + ikA_2]v^e dV = \rho^o \omega^2 \int_{\pi_o} \delta v^{eT} N^T N v^e dV \tag{30}$$

Upon integration using three-point Gauss quadrature method and applying the boundary conditions,

$$[K_1^e + ik(K_2^e) + k^2(K_3^e)]v^e = \omega^2 M^e v^e \tag{31}$$

where, $K_1^e = \int_{\pi_o} A_1^T B A_1 dV$, $K_2^e = \int_{\pi_o} (A_1^T B A_2 - A_2^T B A_1)dV$, $K_3^e = \int_{\pi_o} A_2^T B A_2 dV$,

$$M^e = \int_{\pi_o} \rho^o N^T N dV$$

Developing the global equation,

$$[K_1 + ik(K_2) + k^2(K_3) - \omega^2 M]V = 0 \tag{32}$$

Where V is the global displacement matrix and $K_1 = \bigcup_{e=1}^n K_1^e$, $K_2 = \bigcup_{e=1}^n K_2^e$, $K_3 = \bigcup_{e=1}^n K_3^e$, $M = \bigcup_{e=1}^n M^e$ (n is the number of elements) . In Eq.(32) is a general eigenvalue problem where the eigenvalues are represented by wavenumber k and eigenvectors are represented by V. Phase velocity of the wave is given by the expression,

$$C_p = \frac{\omega}{k} \tag{33}$$

3 RESULTS AND DISCUSSIONS

The eigenvalue problem from the SAFE formulation gives both real numbers and complex numbers. Complex wave numbers correspond to evanescent wave modes which are non-propagating hence, not significant from an application point of view. Hence, the dispersion curves are plotted with the real values of wave numbers which are converted to phase velocity using (33) against the product of frequency and thickness of the plate. To mitigate the effects of material properties from the dispersion curves, we normalize both the phase velocity and frequency-thickness as,

$$\bar{C}_p = C_p \sqrt{\frac{\rho^\circ}{\mu}} \tag{34}$$

$$\bar{fH} = fH \sqrt{\frac{\rho^\circ}{\mu}} \tag{35}$$

For the purpose of analysing the results, we assume wave guide to be made of VHB 4910 with the

following material parameters[20].

Table 1: Material Properties of VHB 4910

Parameters	Magnitude
μ	85.955kPa
λ_m	801.958kPa
ρ°	960 kg/m^3
H	0.001 m

The complete dispersion plot of the above material is shown in Figure 3 with other parameters like fiber orientation, degree of anisotropy, pre-stretch and Gent constant also mentioned in the plot.
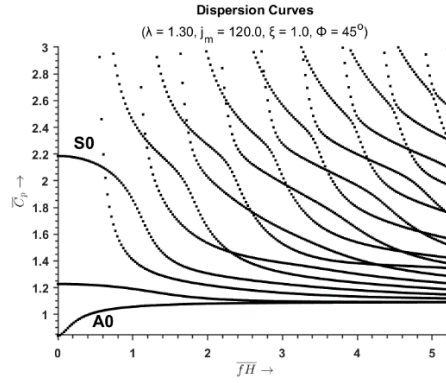

Figure 3: Dispersion plot for the VHB 4910

As seen in Figure 3, the dispersion curve consists of number of modes which are classified as symmetric modes and anti-symmetric modes. The fundamental symmetric and anti-symmetric modes are called S_0 and A_0 modes respectively which are marked in the dispersion curve above. In our analysis, we will be comparing only S_0 and A_0 modes since they are the most important from an application point of view.

3.1 Effect of pre-stretch

In this section, the effect of pre-stretch, given along the ξ_1 direction, on dispersive behaviour of the waves are studied. Keeping all other parameters constant, the values of λ are changed from 1 to 3 with $\lambda = 1$ indicating unstretched condition. The S_0 and A_0 modes are those cases are plotted.

From Figure 4, it can be seen that the A_0 modes are slightly dispersive in the low frequency range $(\overline{fH} < 1)$ whose dispersive nature decreases as the value of the pre-stretch increases with the unstretched case having the most dispersion in the lower frequency regions but over the majority of the frequency-thickness range it is non dispersive since the $\overline{C_p}$ values remain constant over a large range.

On the other hand, the S_0 modes Fig. 5 in are mostly non-dispersive in the lower frequency ranges, but are highly dispersive in the medium frequency range ($1 < \overline{fH} < 2$). Also, the dispersion seems to increase as the value of pre-stretched is increased. Over the higher frequency ranges even though the dispersion is still there, it is very less compared to the medium ranges.
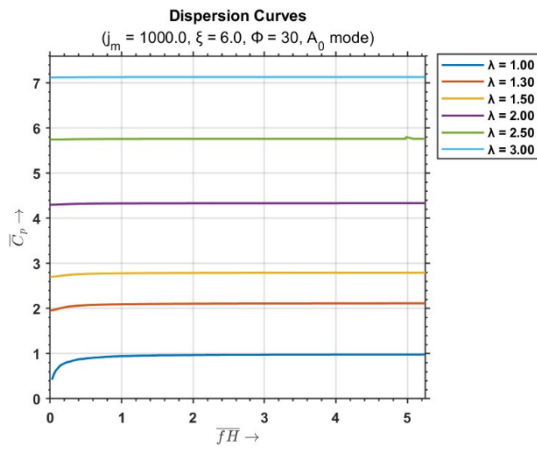
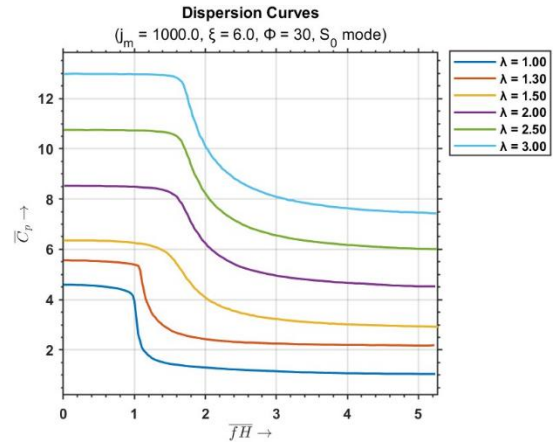Figure 4: Effect of pre-stretch on A_0 mode

Figure 5: Effect of pre-stretch on S_0 mode

3.2 Effect of strain stiffening

In this section, the effect of varying Gent constant j_m is shown while keeping all other parameters constant. j_m is a measure of strain stiffening ability of the material.i.e. an increase in j_m indicates a material with more strain stiffening ability.

In Figure 6, the dispersive nature of A_0 mode is plotted while varying Gent constant. Over the lower frequency ranges, the waves are found to be highly dispersive while over the higher frequencies, the waves are moderately dispersive. Lower value of j_m have higher phase velocity, while for higher values of $j_{m,}$ the values of phase velocity are very similar.

In Figure 7, the dispersive nature of S_0 mode is plotted while varying Gent constant. Over the lower frequency ranges, the waves are found to be only slightly dispersive while over the moderate frequencies, the waves are highly dispersive. Values of j_m i.e., strain stiffening effect does not seem to affect the phase velocity of the S_0 mode.
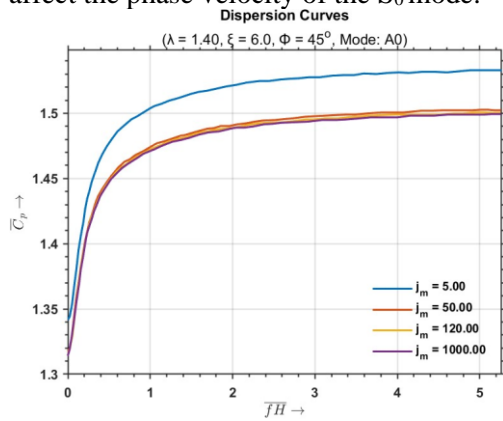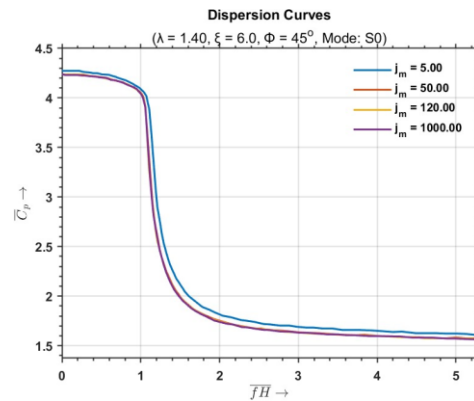

Figure 6: Effect of j_m on A_0 mode

Figure 7: Effect of j_m on A_0 mode

3.3 Effect of fiber orientation

In this section, the orientation of the fibers are varied from 0° to 90^0 while keeping all other parameters constant.
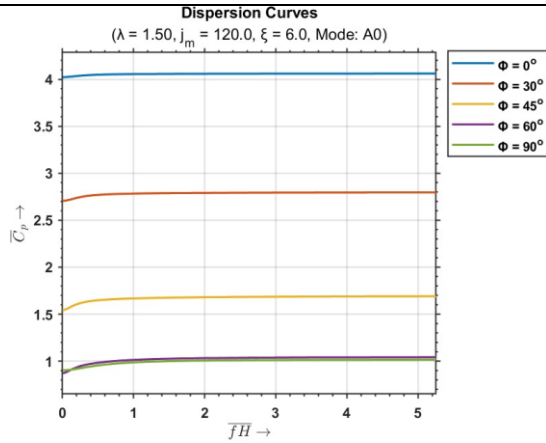
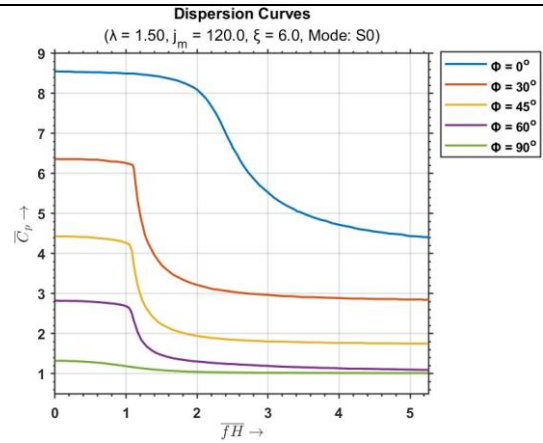Figure 8: Effect of fiber orientation on A_0 mode

Figure 9: Effect of fiber orientation on S_0 mode

The variations on the A_0 mode produced by changing the fiber orientation are shown in Figure 8. The waves are found to be dispersive only at very low frequencies. As ϕ is increased, the magnitude of the wave velocity decreases. It can also be noted that at higher values of ϕ, the values of $\bar{C}_p$ are nearly the same. Similarly, the variations for S_0 mode are shown in Figure 9. We can observe that the S_0 modes are dispersive in the moderate frequency ranges while having comparatively less dispersion in the lower and higher ranges of frequencies.

In the both the fundamental modes, the maximum value of phase velocity occurs when the fibers are oriented with the wave propagation direction.

4   CONCLUSIONS

The work presented establishes a robust computational method for studying how pre-stretch and material parameters influence Lamb modes in compressible, transversely isotropic hyperelastic plate modelled using Gent model. Using the framework of SAFE, in this study, we have been able to study the variation of dispersion nature of the fundamental modes of the Lamb waves propagating through the plates. Various model parameters such as fiber orientation, degree of anisotropy, Gent constant which is a measure of the strain stiffening ability of the material and lastly the pre-stretch applied to the material was discussed.

Going forward, research could extend this SAFE approach to handle wave propagation in anisotropic hyperelastic plates with multiple family of fibers as well. Overall, this Semi-Analytical Finite Element framework offers a way to numerically simulate the effects that nonlinearity and material stiffness have on guided waves in non-linearly elastic structures.

Acknowledgement

REFERENCES

[1]   C. O. Horgan, "The remarkable Gent constitutive model for hyperelastic materials," *International Journal of Non-Linear Mechanics*, vol. 68, pp. 9–16, Jan. 2015, doi: 10.1016/j.ijnonlinmec.2014.05.010.

11

[2]   M. Mohabuth, A. Kotousov, and C.-T. Ng, "Large acoustoelastic effect for Lamb waves propagating in an incompressible elastic plate," *The Journal of the Acoustical Society of America*, vol. 145, no. 3, pp. 1221–1229, Mar. 2019, doi: 10.1121/1.5092604.

[3]   I. Bartoli, A. Marzani, F. Lanza Di Scalea, and E. Viola, "Modeling wave propagation in damped waveguides of arbitrary cross-section," *Journal of Sound and Vibration*, vol. 295, no. 3–5, pp. 685–707, Aug. 2006, doi: 10.1016/j.jsv.2006.01.021.

[4]   M. Hayes and R. S. Rivlin, "Surface waves in deformed elastic materials," *Arch. Rational Mech. Anal.*, vol. 8, no. 1, pp. 358–380, Jan. 1961, doi: 10.1007/BF00277451.

[5]   A. J. Willson, "Wave-propagation in uniaxially-stressed elastic media," *PAGEOPH*, vol. 93, no. 1, pp. 5–18, 1972, doi: 10.1007/BF00875217.

[6]   F. D. Murnaghan, "Finite Deformations of an Elastic Solid," *American Journal of Mathematics*, vol. 59, no. 2, pp. 235–260, 1937, doi: 10.2307/2371405.

[7]   M. Destrade, M. D. Gilchrist, and G. Saccomandi, "Third- and fourth-order constants of incompressible soft solids and the acousto-elastic effect," *The Journal of the Acoustical Society of America*, vol. 127, no. 5, pp. 2759–2763, May 2010, doi: 10.1121/1.3372624.

[8]   R. W. Ogden and D. G. Roxburgh, "The effect of pre-stress on the vibration and stability of elastic plates," *International Journal of Engineering Science*, vol. 31, no. 12, pp. 1611–1639, Dec. 1993, doi: 10.1016/0020-7225(93)90079-A.

[9]   E. V. Nolde, L. A. Prikazchikova, and G. A. Rogerson, "Dispersion of Small Amplitude Waves in a Pre-Stressed, Compressible Elastic Plate," *Journal of Elasticity*, vol. 75, no. 1, pp. 1–29, Apr. 2004, doi: 10.1023/B:ELAS.0000039920.67766.d3.

[10]   P. Kayestha, A. C. Wijeyewickrema, and K. Kishimoto, "Wave propagation along a non-principal direction in a compressible pre-stressed elastic layer," *International Journal of Solids and Structures*, vol. 48, no. 14, pp. 2141–2153, Jul. 2011, doi: 10.1016/j.ijsolstr.2011.03.022.

[11]   Y. Pao and U. Gamer, "Acoustoelastic waves in orthotropic media," *The Journal of the Acoustical Society of America*, vol. 77, no. 3, pp. 806–812, Mar. 1985, doi: 10.1121/1.392384.

[12]   N. Gandhi, J. E. Michaels, and S. J. Lee, "Acoustoelastic Lamb wave propagation in biaxially stressed plates," *The Journal of the Acoustical Society of America*, vol. 132, no. 3, pp. 1284–1293, Sep. 2012, doi: 10.1121/1.4740491.

[13]   M. J. S. Lowe, "Matrix techniques for modeling ultrasonic waves in multilayered media," *IEEE Transactions on Ultrasonics, Ferroelectrics, and Frequency Control*, vol. 42, no. 4, pp. 525–542, Jul. 1995, doi: 10.1109/58.393096.

[14]   F. Chen and P. D. Wilcox, "The effect of load on guided wave propagation," *Ultrasonics*, vol. 47, no. 1, pp. 111–122, Dec. 2007, doi: 10.1016/j.ultras.2007.08.003.

[15]   P. W. Loveday, "Semi-analytical finite element analysis of elastic waveguides subjected to axial loads," *Ultrasonics*, vol. 49, no. 3, pp. 298–300, Mar. 2009, doi: 10.1016/j.ultras.2008.10.018.

[16]   K. Peddeti and S. Santhanam, "Dispersion curves for Lamb wave propagation in prestressed plates using a semi-analytical finite element analysis," *The Journal of the Acoustical Society of America*, vol. 143, no. 2, pp. 829–840, Feb. 2018, doi: 10.1121/1.5023335.

[17]   A. K. Patra, A. K. Sharma, D. M. Joglekar, and M. M. Joglekar, "A Semi-Analytical Finite Element Framework for Lamb Waves in Soft Compressible Plates Considering Strain Stiffening Effect," *Int. J. Appl. Mechanics*, vol. 15, no. 01, p. 2250102, Jan. 2023, doi: 10.1142/S1758825122501022.

[18]   Y. Yang, C. Fu, and F. Xu, "A finite strain model predicts oblique wrinkles in stretched anisotropic films," *International Journal of Engineering Science*, vol. 155, p. 103354, Oct. 2020, doi: 10.1016/j.ijengsci.2020.103354.

[19]   A. Dorfmann and R. W. Ogden, "Electroelastic waves in a finitely deformed electroactive material," *IMA Journal of Applied Mathematics*, vol. 75, no. 4, pp. 603–636, Aug. 2010, doi: 10.1093/imamat/hxq022.

[20]   S. Jemioło, A. Franus, and W. Domański, "Scope of Application of the Murnaghan Hyperelastic Model for Elastomers".

[21] Sharma, A.K., Joglekar, D.M. and Joglekar, M.M., 2024. Propagation of the fundamental Lamb modes in strain stiffened hard-magnetic soft plates. *Journal of Applied Mechanics*, *91*, pp.061007-1.

[22] Patra, A.K., Sharma, A.K., Joglekar, D.M. and Joglekar, M.M., 2023. Propagation of fundamental Lamb modes along the non-principal axes of strain-stiffened soft compressible plates: A numerical investigation. *The Journal of the Acoustical Society of America*, *153*(2), pp.1331-1346.

[23] Patra, A.K., Khurana, A. and Kumar, D., 2024. Modeling and analysis of a thermo-electro-magneto-viscoelastic actuator. International Journal of Applied Mechanics, 16(02), p.2450015.

[24] Kumar, A., Khurana, A., Patra, A.K., Agrawal, Y. and Joglekar, M.M., 2023. Electromechanical performance of dielectric elastomer composites: Modeling and experimental characterization. *Composite Structures*, *320*, p.117130.